Separation of CO_2/N_2 Mixtures Using MFI-Type Zeolite Membranes

M. P. Bernal, J. Coronas, M. Menéndez, and J. Santamaría
Dept. of Chemical and Environmental Engineering, Faculty of Science, University of Zaragoza, 50009 Zaragoza, Spain

MFI-type zeolite (ZSM5) membranes were prepared on alumina and stainless steel tubular supports and tested for the separation of CO_2/N_2 mixtures. The effect of several operating variables (temperature, feed and permeate pressures, feed composition, use of sweep gas, presence of water in the feed, membrane module configuration) was investigated. The separation between CO_2 and N_2 takes place because of the preferential adsorption of CO_2, which hinders the permeation of N_2 through the zeolite pore network. The best results in this work were obtained with a Na-ZSM5 membrane, and using a large pressure gradient. In this case, a permeation flux as large as 9.2 kg/($m^2 \cdot h$) [permeance of 2.6×10^{-6} mol/($m^2 \cdot s \cdot Pa$)] with a CO_2/N_2 separation factor of 13.7 was obtained.
 AIChE J, 50: 127–135, 2004
Keywords: zeolite membrane, ZSM5, CO_2/N_2 separation, CO_2 permeation

Introduction

The report issued by the Intergovernmental Panel on Climate Change (IPCC) (2001) indicates that the concentration of CO_2 in the atmosphere increased from approximately 280 ppmv in preindustrial times to an average of 367 ppmv in 1999, a 31% increase. According to the IPCC, this concentration has not been exceeded, at least during the last 420,000 years, and this increase is mainly a consequence of the use of fossil fuels. Several international efforts (most notably the Kyoto Protocol) are aimed at curbing CO_2 emissions, although achieving this in practice poses formidable technical and economic problems (Armor, 1997), especially for the so-called end-of-pipe solutions. Among the biggest challenges is the need to concentrate and purify the CO_2 present in the exit streams of both fixed and mobile sources before potential CO_2 removal alternatives such as conversion into useful chemicals can be implemented.

Membrane separation has often been advocated as a suitable method for CO_2 separation from gas-phase streams due to the relatively low energy consumption involved. While polymeric membranes show interesting selectivities in the separation of CO_2 from air, many of the possible CO_2 removal applications would involve relatively high temperatures and/or pressures. Thus, inorganic membranes such as zeolitic membranes are being considered as alternative candidates, in view of their higher thermal, mechanical, and chemical stability.

Zeolite membranes are a kind of microporous inorganic membranes that have been used in a wide variety of applications such as the separation of isomers (Giroir-Fendler et al., 1996; Funke et al., 1997; Nomura et al., 1997; Coronas et al., 1997; Vroon et al., 1998; Xomeritakis et al., 2001), gas mixtures (Kusakabe et al., 1998a, b; Lovallo et al., 1998; van den Broeke et al., 1999; Poshusta et al., 2000), pervaporation of alcohol–water mixtures (Kita, et al., 1995; Kondo et al., 1997; Sano et al., 1997). The affinity of the permeating molecules toward the zeolite material, and the difference between the size of these molecules and that of the membrane pores, are the factors that play the key roles in these separations. Most of the zeolitic membranes investigated to date belong to the MFI type (silicalite and ZSM5), although other membrane materials, such as mordenite and zeolites A and Y, have also been studied.

In the case of the separation of CO_2/N_2 mixtures using zeolite membranes, Kusakabe et al. (1997, 1998a, 1999) have probably reported the best results using faujasite-type zeolite (X and Y) membranes. For instance, at 303 K they reported a CO_2 permeance of $1.5 \cdot 10^{-7}$ mol/($m^2 \cdot s \cdot Pa$) and a CO_2/N_2 separation factor of 100 on a NaY membrane (Kusakabe et al.,

Correspondence concerning this article should be addressed to J. Santamaría at iqcatal@posta.unizar.es.

1997). MFI membranes have yielded considerably lower CO_2/N_2 separation factors. Nevertheless, their use in the separation of CO_2/N_2 mixtures is also being investigated (Lovallo et al., 1998; Ando et al., 1998; Masuda et al., 1998; Mase et al., 1998; van den Broeke et al., 1999; Bernal et al., 2002), due to their low Al content, which gives these membranes a good reproducibility and chemical stability. Probably, the best results with MFI membranes have been reported by Ando et al. (1998), who found a separation factor of 25.5 at a CO_2 permeance of $6.6 \cdot 10^{-7}$ mol/($m^2 \cdot s \cdot Pa$). Also, membranes made of pseudozeolites such as SAPO-34 (a chabazite analog) have shown a good performance in this system (Poshusta et al., 2000). A table is given at the end of the results and discussion section comparing the values in the literature and those of this work.

CO_2 has a stronger electrostatic quadrupole than N_2, leading to a more intense interaction of CO_2 with the zeolite material, which translates into a preferential adsorption of CO_2 in CO_2/N_2 mixtures. Thus, it can be expected that surface diffusion of CO_2 would make a significant contribution to its permeation, while at the same time adsorbed CO_2 would reduce the N_2 permeation flux through the membrane; both factors would lead to selective CO_2/N_2 separations (Kusakabe et al., 1997; Lovallo et al., 1998; van den Broeke et al., 1999; Poshusta et al., 2000; Bernal et al., 2002). Dunne et al. (1996a, b) reported that at 300 K, the CO_2 and N_2 isosteric heats of adsorption at the limit of zero coverage increase in the order silicalite $<$ H-ZSM5 $<$ Na-ZSM5, and that for Na-ZSM5 (Si/Al = 30) these were as high as for NaX (Si/Al = 1.23). The fact is that Na^+ ions provide the strongest electric field within the pore. However, at high loadings the effects are less pronounced, and the adsorption heat is similar for silicalite, H-ZSM5, and Na-ZSM5.

In this work we investigate the application of ZSM5 zeolite membranes of different characteristics to the selective separation of CO_2 from its mixtures with N_2. The aim of the study is to assess the effect of different operation variables on the separation performance of the membranes, and to relate the results obtained to the adsorption-controlled separation mechanism just discussed. Molecular sieving (i.e., operation in the size-exclusion regime) is not expected to play a role in the system investigated, due to the close kinetic diameters of the molecules involved ($d_{k,CO_2} = 0.33$ nm; $d_{k,N_2} = 0.37$ nm), and the fact that they are both considerably smaller than the MFI pore size (ca. 0.55 nm).

Experimental

The ZSM5 membranes were prepared on alumina (SCT) and stainless steel (Mott) commercial supports, of 200-nm and 500-nm nominal pore diameters, respectively. The length of the porous wall was between 4 and 5 cm, depending on the membrane, and the inner and outer diameters of the tubes were 6.5 and 10 mm, respectively. Na-ZSM5 membranes were prepared using the gel described by Coronas et al. (1997), with the following molar composition: 21 SiO_2: 987 H_2O: 3 NaOH: 1 TPAOH: 0.105 $Na_2Al_2O_4$. ZSM5 membranes without Na in their structure (H-ZSM5) were synthesized using the following gel: 19.46 SiO_2: 438 H_2O: 1 TPAOH: 0.0162 Al_2O_3 (Tuan et al., 1999). A third type of ZSM5 membrane, boron-substituted ZSM5, (B-ZSM5) was prepared with the following gel: 19.46 SiO_2: 438 H_2O: 1.55 TPAOH: 0.195 $B(OH)_3$ (Tuan et al., 2000). TPAOH is tetrapropylammonium hydroxide.

Two different procedures were employed to prepare the membranes. In procedure (a) the tubular support was wrapped with Teflon tape on the outside and introduced into the autoclave, which was then filled with the respective gel. In procedure (b) a first synthesis was carried out with procedure (a), in order to deposit zeolite crystals in the support. Subsequent synthesis were carried out as follows: the support was wet and filled with the synthesis gel, then plugged with Teflon caps and introduced in an autoclave containing 3 cm^3 of water. In both procedures (a) and (b), the autoclave was placed in a convection oven at 443 K for periods between 8 and 72 h. The synthesis cycle was repeated until a membrane impermeable to N_2 under a pressure gradient of 200 kPa was obtained. The template was then removed by heating up to 753 K at 1 K/min and then maintaining the final temperature for 8 h. The synthesized membranes have a thickness in the range of 5 μm to 80 μm, depending on the synthesis conditions and type of support, as shown in previous studies from our laboratory (Bernal et al., 2000; Piera et al., 1998) and of other groups using similar synthesis procedures (Coronas et al., 1997; Tuan et al., 1999, 2000).

Permeation experiments were carried out by placing the membrane in a stainless steel module, where it was sealed with silicone O-rings. The module was heated by means of an electrical oven, except in some experiments where a cryogenic bath was employed to operate at subambient temperatures. A CO_2/N_2 mass-flow controlled stream was fed into the tube side (retentate), while the permeate side was either kept at a lower pressure or flushed with sweep gas to create the necessary driving force. For the experiments with sweep gas, a He mass-flow controlled stream was fed to the shell side (permeate). A back-pressure regulator at each membrane side was used to control the total pressure and the pressure difference across the membrane (ΔP). When water vapor was also cofed, the CO_2/N_2 feed stream was first bubbled through a water saturator kept at a constant temperature. Before setting them in the permeation module, the membranes were heated to 623 K at a rate of 1 K/min, and then kept at this temperature for 4–8 h in order to remove any adsorbed species.

The exit streams from both retentate and permeate sides were analyzed by on-line gas chromatography. The CO_2/N_2 separation factor (α_{CO_2/N_2}) given below for mixtures after reaching steady-state conditions was calculated as follows

$$\alpha_{CO_2/N_2} = \frac{y_{CO_2}/y_{N_2}}{x_{CO_2}/x_{N_2}}$$

where y and x are, respectively, the molar fractions at the exit of the permeate and retentate streams. The permeation flux (PF) is usually given in cm^3(STP)/min, and sometimes in kg/($m^2 \cdot$ h). Mass-balance closures for the different species based on the composition and flow rate of the feed and the two exit streams were better than 5% for the experiments reported in this work. Finally, some temperature programmed permeation experiments were also carried out, using the experimental system described elsewhere (Bernal et al., 2002).

The stability of the membranes used in this work was remarkable. Thus, for instance, membrane B-ZSM5-1 was kept

Table 1. Properties of the Membranes Used in this Work

Membrane	Support	Synthesis Time (h)	Synthesis Procedure	N_2 Permeance [mol/(m^2 · s · Pa)]	N_2/SF_6 Ideal Selectivity
Na-ZSM5-1	Stainless steel	8/15/8		1.7×10^{-7}	33
Na-ZSM5-2	Stainless steel	15/8/15/8	b	3.1×10^{-7}	8
H-ZSM5-1	Stainless steel	72	a	1.2×10^{-8}	5.2
H-ZSM5-2	α-Al_2O_3	72	a	6.1×10^{-8}	71
H-ZSM5-3	α-Al_2O_3	72	a	8.2×10^{-9}	9.9
H-ZSM5-4	α-Al_2O_3	72	a	1.5×10^{-7}	30
H-ZSM5-5	α-Al_2O_3	72	a	1.9×10^{-7}	10
H-ZSM5-6	α-Al_2O_3	72	a	1.9×10^{-7}	11
H-ZSM5-7	α-Al_2O_3	72	a	9.3×10^{-8}	14
H-ZSM5-8	α-Al_2O_3	72	a	4.4×10^{-8}	26
H-ZSM5-9	Stainless steel	72	a	1.4×10^{-8}	3.5
B-ZSM5-1	Stainless steel	20/20/20	b	5.2×10^{-8}	45
B-ZSM5-2	Stainless steel	20/20/20	b	1.3×10^{-7}	25
B-ZSM5-3	Stainless steel	20/20/20	b	6.4×10^{-8}	19
B-ZSM5-4	Stainless steel	20/20/20	b	4.8×10^{-8}	24

Note: Permeances at 300 K.

under operation for more than 700 h, including several 473–623 K thermal treatments. After this period of time neither the CO_2/N_2 separation factor nor the CO_2 permeation flux changed significantly.

Results and Discussion

Some key characteristics of the membranes tested in this work are shown in Table 1. The N_2/SF_6 ideal selectivity (ratio of single gas permeances) is sometimes used as a membrane quality indicator. However, the relationship between ideal selectivity and membrane performance is not univocal, even for membranes of the same type, and this parameter must be used with caution (Coronas et al., 1997) and often only in a qualitative way. This is especially true for adsorption-controlled separations.

CO_2 adsorption is relatively weak on MFI zeolites [ΔH_{ads} = 27.5, 50, and 38 kJ/mol for silicalite, Na-ZSM5 and H-ZSM5, respectively, at 300 K and zero load limit (Dunne et al., 1996b)]. In spite of this, adsorbed CO_2 could still be expected to block the pass of other gases with a weaker adsorption on MFI membranes, giving rise to selective separations. Among these gases are N_2, H_2, and He, whose heats of adsorption on silicalite are, respectively, 13.8, 5.9, and nearly 0 kJ/mol at 300 K (Bakker et al., 1997).

Table 2 shows some of the CO_2/N_2 separation results obtained in this work using H-ZSM5 membranes. Although all the membranes show separation factors above the Knudsen level (α_K,CO_{2/N_2} = 0.8), it can be seen that only moderate values were obtained, except for membrane H-ZSM5-3, which reached 4.70. This could be expected, in view of the low heat of adsorption for CO_2 on H-ZSM5 zeolites, as seen earlier. It also indicates that CO_2/N_2 is a difficult separation, and high-quality (i.e., nearly defect-free) membranes are necessary to obtain a good separation selectivity.

Influence of temperature

Given the adsorption behavior of CO_2, its permeance-temperature curve is expected to show a trend similar to that of light hydrocarbons, with a maximum at low temperatures followed by a minimum at a higher temperature. Figure 1 shows this expected behavior in the temperature-programmed permeation curves obtained at different CO_2 pressures for membranes Na-ZSM5-2 and B-ZSM5-1. Both membranes were prepared by the same synthesis procedure on stainless steel supports. However, the temperature of the minimum for membrane Na-ZSM5-2 is higher than for membrane B-ZSM5-1, at any feed pressure. This difference can be explained in terms of the concentration of defects in both membranes. The viscous and Knudsen contributions to the permeation flux decrease with temperature, while activated diffusion, typical of transport in micropores, increases. In a membrane with a higher concentration of defects (nonzeolitic pores), a higher temperature will be needed to compensate the viscous and Knudsen contributions, and as a consequence, a displacement of the minimum to higher temperatures would take place (Poshusta et al., 1999). Thus, the results in Figure 1 would indicate a higher quality (lower concentration of defects) for membrane B-ZSM5-1. This is in agreement with the N_2/SF_6 ideal selectivity values (Table 1), which were 45 for B-ZSM5-1 and 8 for Na-ZSM5-2.

On the other hand, after the minimum in the permeance, activated diffusion is the dominant transport mechanism. An Arrhenius-type plot gives a good fit for every set of data ($R >$ 0.9997 in all cases), and apparent activation energies can thus be calculated. The values are given in Table 3, and it can be seen that they are higher for the B-ZSM5-1 membrane (18–22 kJ/mol) compared to membrane Na-ZSM5-2 (10–17 kJ/mol). Since higher apparent activation energies indicate a lower concentration of defects (Bernal et al., 2002), this result again confirms the higher quality of the B-ZSM5-1 membrane.

Table 2. α_{CO_2/N_2} and CO_2 PF for Several H-ZSM-5 Membranes

Membrane	HZSM5-1	HZSM5-3	HZSM5-4	HZSM5-5	HZSM5-6	HZSM5-7	HZSM5-8	HZSM5-9
α_{CO_2/N_2}	2.30	4.70	1.84	1.96	1.87	1.71	2.00	1.85
CO_2 PF cm^3(STP)/min	1.4	2.9	0.8	18.8	23.6	5.9	4.0	7.3

Note: Temperature = 300 K. Feed: CO_2/N_2 = 50/50 kPa; 200 cm^3(STP)/min. He sweep gas = 100 cm^3(STP)/min; permeate pressure = 100 kPa.

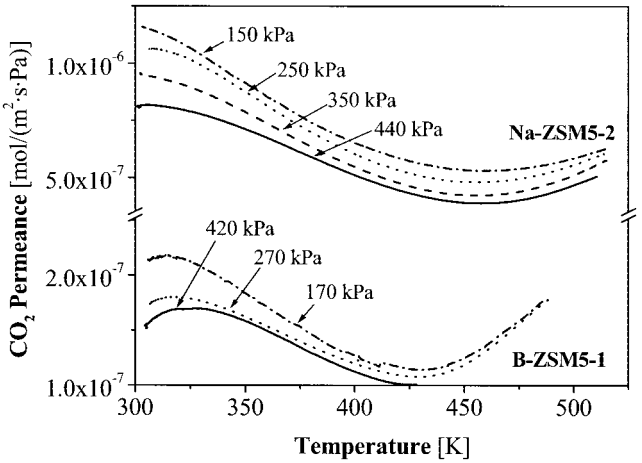

Figure 1. CO_2 single gas permeances for different retentate pressures as a function of temperature for membranes B-ZSM5-1 and Na-ZSM5-2.

Feed: CO_2 = 200 cm^3(STP)/min. Permeate pressure = 100 kPa. Retentate pressures are indicated in the figure.

Figure 1 also shows a decrease in permeance for both membranes when the CO_2 pressure at the retentate side increases. This can be explained as the result of an adsorption-controlled permeation mechanism. Since pure CO_2 is fed to the permeation unit, at any of the pressures used the surface coverage of CO_2 into the retentate side is already considerable and close to saturation levels. Further increases in the partial pressure of CO_2 increase the permeation flux, but the increase is not enough to compensate for the higher pressure difference, and the permeance (permeation flux normalized per unit of pressure difference) decreases.

Figure 2 shows the CO_2 permeation flux and the CO_2/N_2 separation factor as a function of retentate pressure for one of the boron-containing membranes (B-ZSM5-1) at a constant permeate pressure of 100 kPa and several temperatures (300, 373, and 473 K). As expected for an adsorption-controlled process, when the temperature increased from 300 K to 473 K, the amount of CO_2 adsorbed in the membrane pores decreased and so did the CO_2/N_2 separation factor (see Figure 2b). Also, at any temperature tested, the separation factor increased with the retentate pressure. The adsorption-controlled permeation also accounts for this effect: as the retentate pressure increased, both the average CO_2 partial pressure in the membrane and the amount of CO_2 adsorbed in the membrane pores increased, giving rise to a higher CO_2 coverage at the retentate side. This

Table 3. Apparent Activation Energies of Permeation for Membranes Na-ZSM5-2 and B-ZSM5-1 at Different Retentate Pressures and Atmospheric Pressure in the Permeate Side

Na-ZSM5-2		B-ZSM5-1	
P_{ret} (kPa)	E_{act} (kJ/mol)	P_{ret} (kPa)	E_{act} (kJ/mol)
150	10.1	170	18.3
250	12.9	270	21.6
350	17.4	—	—
440	16.2	—	—

Note: Temperature range: 453–488 K (B-ZSM5-1) and 483–513 K (Na-ZSM5-2).

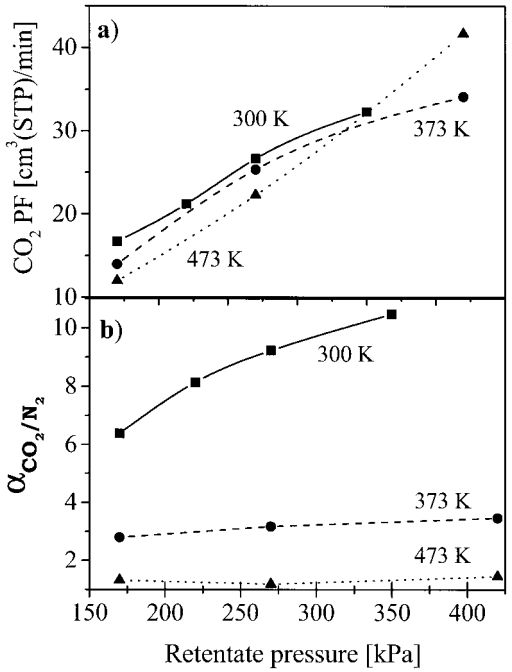

Figure 2. (a) CO_2/N_2 separation factor (α_{CO_2/N_2}) and (b) CO_2 permeation flux (PF) as a function of the total pressure at the retentate for membrane B-ZSM5-1 at several temperatures.

Feed: CO_2/N_2 = 100/100 cm^3(STP)/min. No sweep gas was used; permeate pressure = 100 kPa.

increased both the separation factor (by blocking N_2 access to the zeolite pores) and the CO_2 permeation flux.

Finally, with the aim of establishing the temperature where the highest CO_2/N_2 selectivity occurred, the permeation module was placed in a subambient bath capable of lowering the temperature to 238 K. As shown in Figure 3, the maximum

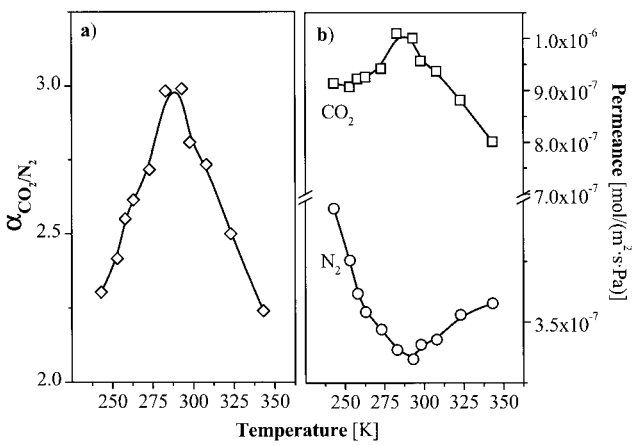

Figure 3. (a) CO_2/N_2 separation factor (α_{CO_2/N_2}) and (b) CO_2 and N_2 permeances as a function of temperature at the retentate for membrane Na-ZSM5-2.

Feed: CO_2/N_2 = 100/100 cm^3(STP)/min; permeate pressure = 100 kPa, retentate pressure = 200 kPa. No sweep gas was used.

Table 4. α_{CO_2/N_2} and CO_2 PF of Membrane B-ZSM5-1 at Different Feed Flow Rates

Feed Flow Rate [cm³(STP)/min]	CO_2 P_{ret}-P_{perm} (kPa)	CO_2 PF [cm³(STP)/min]	α_{CO_2/N_2}
205	60	19.2	6.8
	149	40.1	10.8
280	63	19.3	7.7
	159	42.3	11.2
400	64	19.3	7.5
	167	42.6	11.9

Note: Temperature = 300 K. Feed: CO_2/N_2 = 85/85–210/210 kPa. He sweep gas = 100 cm³(STP)/min; permeate pressure = 100 kPa.

CO_2/N_2 separation factor for Na-ZSM5-2 membrane was observed at 288 K. Note that 288 K is also the temperature found for the CO_2 permeance maximum and for the N_2 permeance minimum. That is, as observed in the separation of butanes (Vroon et al., 1998; Coronas et al., 1997), the maximum selectivity is obtained at a temperature where the combination of adsorption and diffusion produces an efficient blockage of the less strongly adsorbed species and at the same time allows a sufficiently high permeance of the favored one.

Influence of feed flow rate

Table 4 shows the performance of membrane B-ZSM5-1 in two different ranges of partial pressure gradient (60–64 and 149–167 kPa of CO_2), at different values of the feed flow rate [from 205 to 400 cm³(STP)/min]. The trend is similar in the two cases, with an increase of the separation factor and the permeation flux of CO_2 as the feed flow rate increased. This is expected since for the lower flow rates employed the permeation of CO_2 causes a significant decrease on the partial pressure of CO_2 at the retentate [such as when the partial pressure gradient is in the 149–167-kPa interval, the permeation flux of CO_2 is in the 40–43-cm³(STP)/min range, representing between 10 and 20% of the total CO_2 feed]. This decreases both the amount of CO_2 adsorbed on the membrane pores and the driving force for the CO_2 transport, giving rise to the effects observed.

An additional factor is the back-permeation of He from the shell side (data not shown). This takes place mainly through intercrystalline pores and is little affected by the retentate feed flow rate. Since the measured back-permeation flux was relatively constant [8.0 to 12 cm³(STP)/min of He throughout the different conditions of Table 4], the dilution effect produced was more important at the lowest end of the feed flow rates employed.

Influence of retentate pressure and sweep-gas flow rate

The effect of the feed pressure was shown in Figure 2 for membrane B-ZSM5-1 at different temperatures, and is shown in Figure 4 for different membranes and operation modes. Experiments without sweep gas are represented by closed symbols and those where He sweep gas was used with open symbols. Again, it can be seen that the separation factor increases with the retentate pressure (up to a pressure of 420 kPa) in experiments with and without sweep gas on the permeate side. The same trend was observed by van den Broeke et al. (1999) using a silicalite membrane and sweep gas at the permeate side, although the effects observed were of a smaller

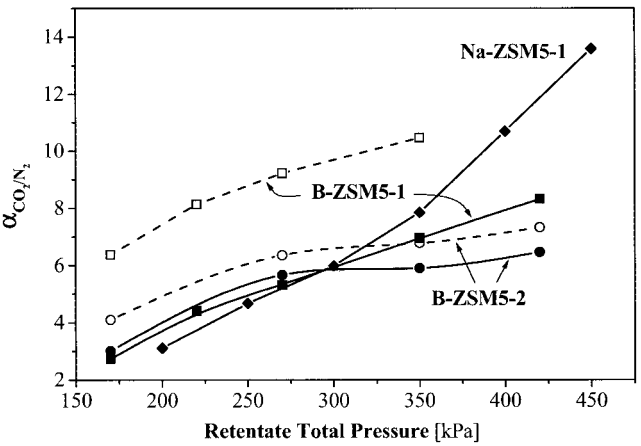

Figure 4. CO_2/N_2 separation factor (α_{CO_2/N_2}) as a function of retentate total pressure for several membranes.

Temperature = 300 K. Feed: CO_2/N_2 = 100/100 cm³(STP)/min. Closed symbols for experiments without sweep gas; open symbols for experiments with He sweep gas = 100 cm³(STP)/min); permeate pressure = 100 kPa.

magnitude. It is interesting to note that in our case, for the same retentate pressure, the separation factor obtained with a good-quality membrane such as B-ZSM5-1 was higher when a sweep gas was used. Flowing a sweep gas at the permeate side could in principle have several beneficial effects. On the one hand, it would increase the driving force for permeation by lowering the CO_2 concentration at the permeate side. Furthermore, higher sweep-gas flow rates would also increase the turbulence and the mass-transfer coefficient at the permeate side, accelerating desorption of the permeated species. Finally, if viscous flow exists in intercrystalline pores, the back-permeation of the sweep gas would increase the separation factor by reducing the

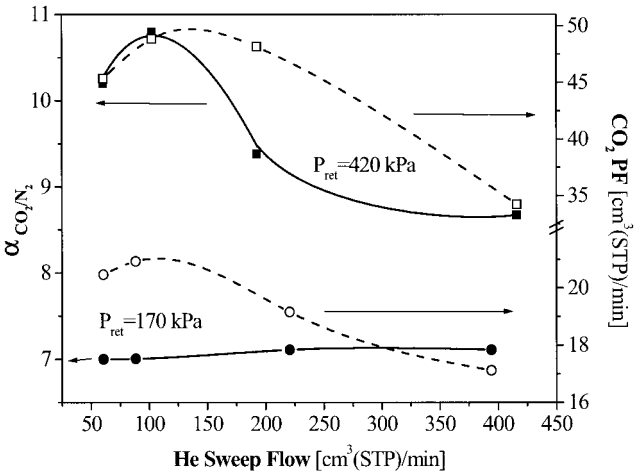

Figure 5. CO_2/N_2 separation factor (α_{CO_2/N_2}) and CO_2 Permeation flux (PF) and as a function of He sweep flow for membrane B-ZSM5-1.

Temperature = 300 K. Feed: CO_2/N_2 = 100/100 cm³(STP)/min. Permeate pressure = 100 kPa. Open symbols for CO_2 fluxes and closed symbols for CO_2/N_2 separation factors. Squares for experiments with a retentate pressure of 420 kPa and circles for 170 kPa.

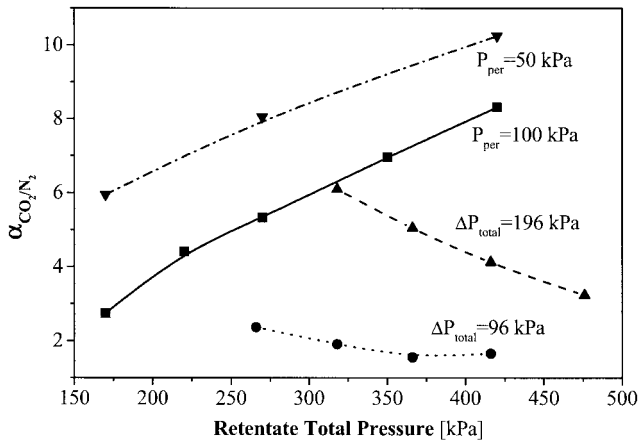

Figure 6. CO_2/N_2 separation factor (α_{CO_2/N_2}) as a function of retentate total pressure for membrane B-ZSM5-1 for experiments run with either constant permeate pressures or with constant total pressure gradients.

Temperature = 300 K. Feed: CO_2/N_2 = 100/100 cm^3(STP)/min. He sweep gas was not employed.

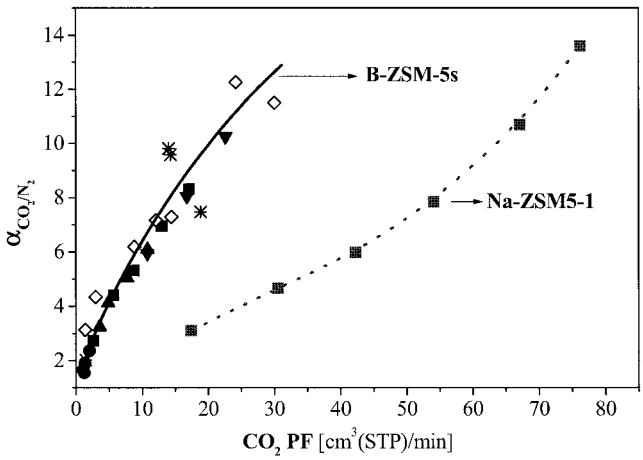

Figure 7. CO_2/N_2 separation factor (α_{CO_2/N_2}) as a function of CO_2 permeation flux (PF) for membranes B-ZSM5-s and Na-ZSM5-1.

Same conditions as in Figure 6. Symbols for B-ZSM5 membranes: permeate pressure 100 kPa and variable retentate total pressures for membrane B-ZSM5-1 (■), B-ZSM5-3 (*), and B-ZSM5-4 (◇); permeate pressure 50 kPa and variable retentate total pressures for membrane B-ZSM5-1 (▼); variable permeate and retentate total pressures with a constant total pressure gradient of 96 kPa (●) and 196 kPa (▲).

permeation flux in these pores. However, Figure 5 shows that there is an optimum value of the sweep-gas flow rate on both the CO_2 permeation flux and the CO_2/N_2 separation factor. This optimum is around 100 cm^3(STP)/min for the experiments in Figure 5. At higher values of the sweep-gas flow rate, the concentration of CO_2 in the zeolite pores decreases beyond the value necessary to maintain an efficient pore blockage, and the separation factor decreases.

When considering the effect of the retentate pressure, it is interesting to compare the results obtained under different operation modes. Figure 6 plots the CO_2/N_2 separation factor as a function of retentate pressure for membrane B-ZSM5-1 in experiments without a sweep gas at the permeate side. Two operating modes were used: a constant permeate pressure (50 or 100 kPa), and a constant pressure gradient across the membrane (96 or 196 kPa). It can be seen that the separation factor increased with the retentate pressure only for the experiments with a constant permeate pressure. This is consistent with the behavior just discussed, where a higher CO_2 pressure increases the amount of adsorbed CO_2 and blocks N_2 permeation more efficiently. The situation is completely different for the experiments with a constant pressure gradient across the membrane, where the separation factor decreases markedly with the retentate pressure. In this case, as the retentate pressure increases, the permeate pressure must also increase to maintain the total pressure gradient. Since a sweep gas is not used, this leads to a reduction in the driving force for CO_2 permeation. For instance, in Figure 6 for a pressure gradient of 196 kPa, the CO_2 partial-pressure gradients for the first and second experimental points (at retentate total pressures of 318 and 366 kPa) are 48.6 and 37.5 kPa, respectively. The decrease in the partial-pressure gradient reduces the CO_2 permeation flux, giving a lower separation factor.

Figure 7 plots the CO_2/N_2 separation factor as a function of the CO_2 permeation flux for the different B-containing membranes used in this work. The data corresponding to the best Na-ZSM5 membrane are also included for comparison. It is interesting to note that a very good correlation is achieved, and the data obtained with all the B-ZSM5 membranes can be fitted with a single curve. It can be seen that both B-ZSM5 membranes and Na-ZSM5 membranes are capable of reaching values of the CO_2/N_2 separation factor above 10, while giving

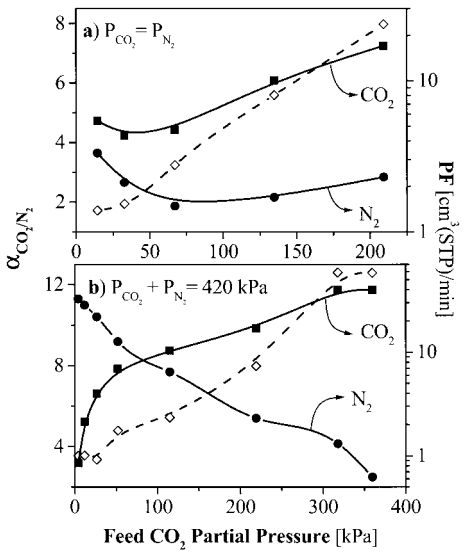

Figure 8. CO_2 permeation flux (PF) and CO_2/N_2 separation factor (α_{CO_2/N_2}) as a function of the CO_2 partial pressure in the feed for membrane B-ZSM5-1.

Temperature: 300 K, feed flow rate: 200 cm^3(STP)/min, He sweep gas was not employed; permeate pressure: 100 kPa, retentate pressure: 420 kPa. (a) Experiments run with the same partial pressures of CO_2 and N_2 in the feed, with He as balance ($P_{CO_2} + P_{N_2} + P_{He}$ = 420 kPa); (b) experiments run without He in the feed ($P_{CO_2} + P_{N_2}$ = 420 kPa).

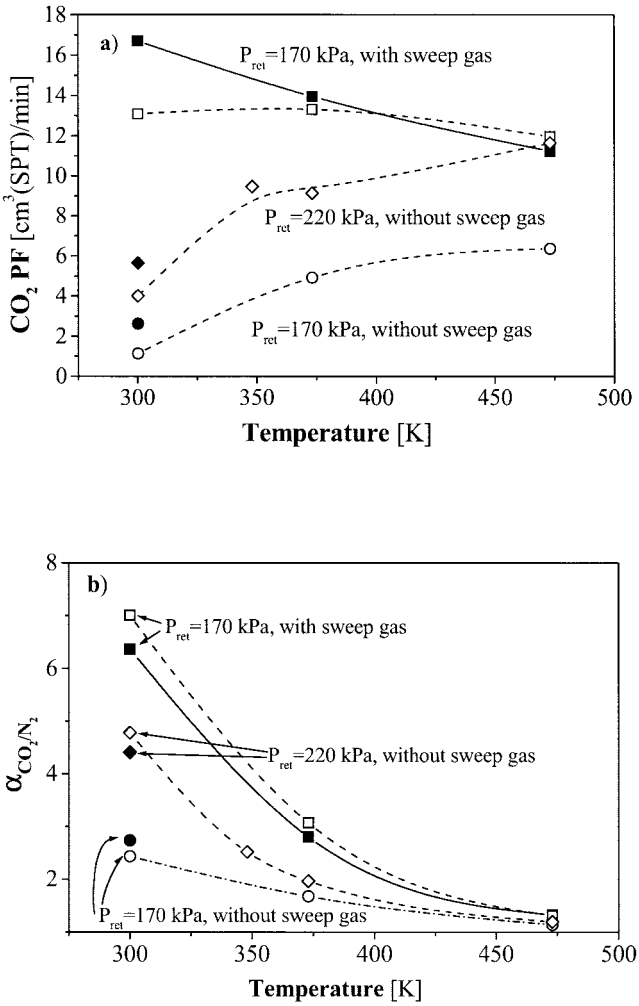

Figure 9. (a) CO_2 permeation flux (PF) and (b) CO_2/N_2 separation factor (α_{CO_2/N_2}) as a function of temperature for membrane B-ZSM5-1 at several retentate pressure and sweep gas conditions.

Feed: CO_2/N_2 = 100/100 (cm^3(STP)/min). He sweep gas (if used) = 100 cm^3(STP)/min; permeate pressure = 1 atm. Open symbols: feed saturated in water, close symbols: dry feed.

reasonable permeation fluxes. This was not possible with H-ZSM5 membranes, as shown earlier. For the case of Na-ZSM5 membranes, it has already been shown that their good performance can be explained by the increased adsorption heat of CO_2 on Na-ZSM5 compared to H-ZSM5 (Dunne et al., 1996b). Regarding the B-ZSM5 membranes, one possible contributing factor could be the lower Brönsted acidity of the resulting MFI membranes, compared to their Al-containing counterparts. Although specific data are not available, it seems reasonable to assume that the lower-acidity B-substituted membranes would interact with CO_2 more strongly than H-ZSM5.

Influence of feed composition

It has been indirectly shown (especially in the experiments with a variable retentate pressure) that the CO_2 partial pressure at the retentate side has a strong influence on membrane performance. In this section, two additional types of experiments are reported for the same membrane (B-ZSM5-1). The results plotted in Figure 8a were obtained with a constant total pressure at the retentate side (420 kPa), and with the same CO_2 and N_2 partial pressures in the feed, with He as a balance. Figure 8b shows results obtained with the same total pressure at the retentate, but in the absence of He (i.e., using binary CO_2/N_2 mixtures as feed). In both cases, the separation factor increases continuously with the CO_2 partial pressure in the feed and there is little difference in the separation factors obtained in Figures 8a and 8b at CO_2 partial pressures above 100 kPa. The CO_2 permeation fluxes are also similar through most of the interval explored. In agreement with previous works, this confirms that the flux of the more strongly adsorbed component is little affected by the partial pressure of weakly adsorbed species, such as N_2. Only at the lowest range of CO_2 partial pressures tested is N_2 able to successfully compete with CO_2 for adsorption sites, and this only occurs when its own partial pressure is high enough. Thus, even when the partial pressure of CO_2 is below 30 kPa, the permeation flux of CO_2 is still higher for the experiment with He present in the feed, that is, where the partial pressures of N_2 and CO_2 are equal.

Effect of humidity

Since it seems likely that in most practical applications CO_2 should be separated from a H_2O-containing gas stream, some experiments were also run to assess the effect of humidity on membrane performance. To this end, an equimolar CO_2/N_2 mixture was bubbled at 300 K through a saturator filled with water. The total pressure in the feed side was 170 kPa or 220 kPa, while the temperature of the membrane was increased from 300 K to 473 K. Figure 9 shows the results obtained with membrane B-ZSM5-1. At room temperature, capillary condensation of water can have a significant influence by blocking small defects and hindering part of the nonselective transport

Table 5. α_{CO_2/N_2}, and CO_2 Partial Pressure Gradient of Membrane B-ZSM5-1 as a Function of the Membrane Module Configuration

Retentate Pressure (kPa)	Feeding Through Zeolite Layer Side			Feeding Through Support Side		
	α_{CO_2/N_2}	CO_2 PF [cm^3(STP)/min]	CO_2 $P_{ret} - P_{perm}$ (kPa)	α_{CO_2/N_2}	CO_2 PF [cm^3(STP)/min]	CO_2 $P_{ret} - P_{perm}$ (kPa)
170	6.37	16.7	62.8	1.67	14.3	65.3
220	8.13	21.2	79.7	1.42	17.2	103
270	9.23	26.7	95.1	1.27	19.2	124
350	10.5	32.3	121	1.18	23.0	162

Note: Temperature = 300 K. Feed: CO_2/N_2 = 100/100 cm^3(STP)/min. He sweep gas = 100 cm^3(STP)/min; permeate pressure = 100 kPa.

Table 6. Some Examples of the Best Results Reported on CO_2/N_2 Separation Using Zeolite Membranes

Membrane	Temp. (K)	CO_2:N_2 in the Feed	α_{CO_2/N_2}	CO_2 PF [kg/(m^2 · h)]	CO_2 Permeance [mol/(m^2 · s · Pa)]	Reference
SAPO-34	300	1:1	16	0.7	$9.8 \cdot 10^{-8}$	Poshusta et al. (2000)
Na-Y	303	1:1	100	1.2	$1.5 \cdot 10^{-7}$	Kusakabe et al. (1997)
Na-Y	303	4:1	5	9.1	—	Clet et al. (2001)
K-Y	313	1:1	30.3	14.3	$1.8 \cdot 10^{-6}$	Kusakabe et al. (1999)
Silicalite	303	1:9	25.5	2.1	$6.6 \cdot 10^{-7}$	Ando et al. (1998)
Silicalite	453	7:3	20	0.2	$1.7 \cdot 10^{-8}$	Lovallo et al. (1998)
Silicalite	303	1:9	10	1.6	$5.0 \cdot 10^{-8}$	Mase et al. (1998)
Silicalite	303	9:1	5.5	5.5	$7.0 \cdot 10^{-8}$	Van den Broeke et al. (1999)
K-ZSM-5	323	1:1	2	0.4	$4.5 \cdot 10^{-8}$	Masuda et al. (1998)
B-ZSM-5	300	6:1	12.6	5.1	$1.9 \cdot 10^{-7}$	This work
Na-ZSM-5	300	1:1	13.7	9.2	$2.6 \cdot 10^{-6}$	This work

through the membrane, causing a decrease in the permeation flux. On the other hand, water may also compete for adsorption sites, and influence transport through the zeolite pores. In our case, without sweep gas and at the lowest temperatures tested, a 29 and 54% decrease in the CO_2 permeation flux was measured for retentate pressures of 220 and 170 kPa, respectively. On the other hand, the existence of water in the feed did not change the separation factor significantly, even at low temperatures (see Figure 9b). In summary, the effect of humidity was small, due to the limited hydrophilicity of ZSM5 membranes.

Effect of the membrane-module configuration

Finally, the influence of the membrane-module feed configuration was also studied, that is, whether the CO_2/N_2 mixture was fed from the retentate side (where the zeolite layer is located) or from the support side. The results are shown in Table 5. In all the cases studied, the CO_2/N_2 separation factor was lower when the mixture was fed from the support side. Van de Graaf et al. (1998) already noticed this fact when studying the separation of ethane/methane mixtures through silicalite membranes. In our case, it can be seen that the decrease in both the CO_2/N_2 separation factor and the CO_2 permeation flux is larger at high retentate pressures, while, as already shown, when the usual configuration was employed the performance of the membrane increased with the retentate pressure. This is due to the fact that the support on which the zeolitic material is synthesized has a wide thickness (1500 μm) compared to that of the zeolite layer (20–40 μm), involving a significant restriction to the permeation flow. Thus, when the CO_2/N_2 mixture was fed from the support side, a lower average CO_2 partial pressure was obtained over the zeolite layer. This reduces the CO_2 concentration in the zeolite pores of the membrane to the zeolite layer, resulting in a less efficient blocking of N_2 permeation.

Conclusions

MFI-type zeolite (ZSM5) membranes prepared using different synthesis procedures on alumina and stainless steel supports were able to selectively separate CO_2 from N_2. The separation is controlled by the preferential adsorption of CO_2 in the zeolite pores, hindering the permeation of N_2. With this description we have been able to explain the effect of the operating variables studied in this work, such as the total pressure of the temperature retentate, CO_2 partial pressure, and sweep-gas flow rate. On the other hand, these membranes can operate in the presence of gas-phase water without loss of separation selectivity, although the CO_2 permeation flux can be reduced significantly.

Comparing the performance of the MFI zeolite membranes used in this work to those reported in the literature with zeolite membranes for this system (Table 6), it can be seen that the MFI membranes show one of the highest permeation fluxes (9.2 kg/(m^2 · h)) and the highest permeance (2.6×10^{-6} mol/(m^2 · s · Pa)], with a respectable separation factor (ca. 14). These interesting features are made possible by the inorganic character of the membranes, enabling them to withstand high pressure gradients.

Acknowledgments

Financial support from DGICYT and DGA (Spain) is gratefully acknowledged.

Literature Cited

Ando, Y., Y. Hirano, S. Mase, and H. Taguchi, "Preparation and Characterization of Monolithic and Planar Elements of Zeolite Membranes," *Proc. ICIM'98,* Nagoya, Japan, p. 124 (1998).

Armor, J. N., "Catalytic Solutions to Reduce Pollutants," *Catal. Today,* **38,** 163 (1997).

Bakker, W. J. W., L. J. P. van den Broeke, F. Kapteijn, and J. A. Moulijn, "Temperature Dependence of One-Component Permeation through a Silicalite-1 Membrane," *AIChE J.,* **43**(9), 2203 (1997).

Bernal, M. P., J. Coronas, M. Menéndez, and J. Santamaría, "Characterization of Zeolite Membranes by Temperature Programmed Permeation and Step Desorption," *J. Membr. Sci.,* **195**(1), 135 (2002).

Clet, G., L. Gora, N. Nishiyama, J. C. Jansen, H. Van Bekkum, and T. Maschmeyer, "An Alternative Synthesis Method for Zeolite Y Membranes," *Chem. Commun.,* **41** (2001).

Coronas, J., J. L. Falconer, and R. D. Noble, "Characterization and Permeation Properties of ZSM-5 Tubular Membranes," *AIChE J.,* **43,** 1797 (1997).

Dunne, J. A., R. Mariwala, M. Rao, S. Sircar, R. J. Gorte, and A. L. Myers, "Calorimetric Heats of Adsorption and Adsorption Isotherms. 1. O_2, N_2, Ar, CO_2, CH_4, C_2H_6 and SF_6 on Silicalite," *Langmuir,* **12,** 5888 (1996a).

Dunne, J. A., M. Rao, S. Sircar, R. J. Gorte, and A. L. Myers, "Calorimetric Heats of Adsorption and Adsorption Isotherms. 2. O_2, N_2, Ar, CO_2, CH_4, C_2H_6 and SF_6 on NaX, H-ZSM-5 and Na-ZSM-5 Zeolites," *Langmuir,* **12,** 5896 (1996b).

Funke, H. H., K. R. Frender, K. M. Green, J. L. Wilwerding, B. A. Sweitzer, J. L. Falconer, and R. D. Noble, "Influence of Adsorbed Molecules on the Permeation Properties of Silicalite Membranes," *J. Membr. Sci.,* **129,** 77 (1997).

Giroir-Fendler, A., J. Peureux, H. Mozzanega, and J. A. Dalmon, "Char-

acterization of a Zeolite Membrane for Catalytic Membrane Reactor Application," *Stud. Surf. Sci. Catal.,* **111,** 127 (1996).
IPCC, "Climate Change 2001: A Scientific Basis," Intergovernmental Panel on Climate Change, J. Houghton, Y. Ding, D. J. Griggs, M. Noguer, P. J. van der Linden, X. Dai, C. A. Johnson, and K. Maskell, eds., Cambridge Univ. Press, Cambridge (2001).
Kita, H., K. Horii, Y. Ohtoshi, and K. Okamoto, "Synthesis of a Zeolite Na-A Membrane for Pervaporation of Water-Organic Liquid-Mixtures," *J. Mater. Sci. Lett.,* **14,** 206 (1995).
Kondo, M., M. Komori, H. Kita, and K. Okamoto, "Tubular-Type Pervaporation Module with Zeolite Na-A Membrane," *J. Memb. Sci.,* **133,** (1997).
Kusakabe, K., T. Kuroda, and S. Morooka, "Separation of Carbon-Dioxide from Nitrogen Using Ion-Exchanged Faujasite-Type Zeolite Membranes Formed on Porous Support Tubes," *J. Membr. Sci.,* **148**(1), 13 (1998a).
Kusakabe, K., T. Kuroda, A. Murata, and S. Morooka, "Formation of a Y-Type Zeolite Membrane on a Porous α-Alumina," *Ind. Eng. Chem. Res.,* **36,** 649 (1997).
Kusakabe, K., T. Kuroda, K. Uchino, Y. Hasegawa, and S. Morooka, "Gas Permeation Properties of Ion-Exchanged Faujasite-Type Zeolite Membranes," *AIChE J.,* **45,** 1220 (1999).
Kusakabe, K., M. Yamamoto, and S. Morooka, "Gas Permeation and Micropore Structure of Carbon Molecular Sieving Membranes Modified by Oxidation," *J. Membr. Sci.,* **149,** 59 (1998b).
Lovallo, M. C., A. Gouzinis, and M. Tsapatsis, "Synthesis and Characterization of Oriented Membranes Prepared by Secondary Growth," *AIChE J.,* **44,** 1903 (1998).
Mase, S., Y. Ando, Y. Hirano, and H. Taguchi, "Planar Type Module with Zeolite (MFI) Membranes," *Proc. ICIM'98,* Nagoya, Japan, p. 652 (1998).
Masuda, T., K. Hashimoto, F. Kapteijn, and J. A. Moulijn, "Selective Permeation of CO_2 from Mixture Gas of CO_2 and N_2 through ZSM-5 Zeolite Membrane," Proc. ICIM'98, Nagoya, Japan, p. 128 (1998).
Nomura, M., T. Yamaguchi, and S. Nakao, "Silicalite Membrane Modified by Counterdiffusion CVD Technique," *Ind. Eng. Chem. Res.,* **36**(10), 4217 (1997).
Piera, E., A. G. Giroir-Fendler, J. A. Dalmon, H. Moueddeb, J. Coronas, M. Menéndez, and J. Santamaría, "Separation of Alcohols and Alcohols/O_2 Mixtures Using Zeolite MFI Membranes," *J. Membr. Sci.,* **142,** 97 (1998).
Poshusta, J. C., R. D. Noble, and J. L. Falconer, "Temperature and Pressure Effects on CO_2 and CH_4 Permeation Through MFI Zeolite Membranes," *J. Membr. Sci.,* **160**(1), 115 (1999).
Poshusta, J. C., V. A. Tuan, E. A. Pape, R. D. Noble, and J. L. Falconer, "Separation of Light Gas Mixtures Using SAPO-34 Membranes," *AIChE J.,* **46,** 4, 779 (2000).
Sano, T., S. Ejiri, K. Yamada, Y. Kawakami, and H. Yanagishita, "Separation of Acetic Acid-Water Mixtures by Pervaporation Through Silicalite Membrane," *J. Membr. Sci.,* **123**(2), 225 (1997).
Tuan, V. A., J. L. Falconer, and R. D. Noble, "Alkali-Free ZSM-5 Membranes: Preparation Conditions and Separation Performance," *Ind. Eng. Chem. Res.,* **38,** 3635 (1999).
Tuan, V. A., J. L. Falconer, and R. D. Noble, "Boron-Substituted ZSM-5 Membranes: Preparation and Separation Performance," *AIChE J.,* **46,** 1201 (2000).
Van de Graaf, J. M., E. van der Bijl, A. Stol, F. Kapteijn, and J. A. Moulijn, "Effect of Operating Conditions and Membrane Quality on the Separation Performance of Composite Silicalite-1 Membranes," *Ind. Eng. Chem. Res.,* **37,** 4071 (1998).
Van den Broeke, L. J. P., W. J. W. Bakker, F. Kapteijn, and J. A. Moulijn, "Transport and Separation Properties of a Silicalite-1 Membrane—II. Variable Separation Factor," *Chem. Eng. Sci.,* **54,** 259 (1999).
Vroon, Z. A. E. P., K. Keizer, A. J. Burggraaf, and H. Verweij, "Preparation and Characterization of Thin Zeolite MFI Membranes on Porous Supports," *J. Memb. Sci.,* **144,** 65 (1998).
Xomeritakis, G., Z. Lai, and M. Tsapatsis, "Separation of Xylene Isomer Vapors with Oriented MFI Membranes Made by Seeded Growth," *Ind. Eng. Chem. Res.,* **40**(2), 544 (2001).

Manuscript received Sept. 2, 2002, and revision received May 20, 2003.